

# Spatio-Temporal Landslide Hazard Mapping Using Coupled Hydrological Model in Mt Umyeon, Seoul

Ananta Man Singh Pradhan, Yun-Tae Kim \*

Department of Ocean Engineering, Pukyong National University, Busan, South Korea

## Email address:

anantageo@hotmail.com (Ananta M. S. P.), yuntkim@pknu.ac.kr (Yun-Tae K.)

\*Corresponding author

## To cite this article:

Ananta Man Singh Pradhan, Yun-Tae Kim. Spatio-Temporal Landslide Hazard Mapping Using Coupled Hydrological Model in Mt Umyeon, Seoul. *Landscape Architecture and Regional Planning*. Vol. 2, No. 3, 2017, pp. 83-88. doi: 10.11648/j.larp.20170203.13

**Received:** July 26, 2017; **Accepted:** August 10, 2017; **Published:** August 25, 2017

---

**Abstract:** Landslide hazard maps are important for risk management and land-use planning in mountainous countries such as Korea. The aim of this study was to produce and evaluate a shallow landslide hazard map using a physically based slope stability model coupling with hydrological models in Mt Umyeon, South Korea. The incorporation of a rainfall frequency–duration relationship of heavy rainfall into the assessment of landslide hazard provides a practical way to include climate information into the estimation of shallow landslide hazard. A GIS-based landslide inventory map of 146 landslide locations was prepared using data from previous reports, aerial photographic interpretation, and extensive field work. And this landslide inventory was used to document sites of instability and to provide a test of model performance by comparing observed landslide locations with model predictions. A combined approach of Quasi-dynamic wetness (QDWI) and infinite slope model was used to prepare landslide hazard maps of different durations i.e. considering 17hr duration with average rainfall intensity (case I), 15hr duration with average rainfall intensity (case II) and the last 2hr duration and average intensity added in case II (case III). The results of the analysis were verified using the landslide location data. Receiver operating curve was used to compare all cases. The case III shows satisfactory agreement between hazard map and the existing data on landslide locations with 82.2% accuracy of the model. The results of this study can therefore be used to mitigate landslide-induced hazards and to plan land-use.

**Keywords:** QDWI, Infinite Slope, Rainfall, Mt Umyeon

---

## 1. Introduction

Landslides constitute a major natural hazard in the Republic of Korea due to the high rates of weathering, abundant rainfall, and infrastructure development. Urban and industrial areas in Korea experienced rapid development from the 1960s to the 1980s, and Korea is currently experiencing changes in climate parameters, including annual temperature and precipitation [1]. Landslides on steep slopes are always a major concern because they can affect lives and inflict economic losses. The occurrence of rainfall-triggered shallow landslides can evolve into debris flows, resulting in high risk where vulnerable targets are involved. Such events are of concern in hydro-geomorphic and natural hazards science because the number of people affected globally. Rainfall induced landslides are usually shallow failures on weathered granite slopes in Korea. The formation and rise of a temporary perched water table, which is in contact with the

less permeable bedrock, increase the pore water pressure and cause a reduction in the shear strength of the soil [2].

Landslide hazard maps represent one of the key elements for landslide risk management and regional planning. Landslide hazard is the probability of the spatial occurrence of a slope failure, given a set of geo-environmental conditions [3]. Many methods have been proposed to evaluate landslide hazard at the basin scale, including statistical classification methods and process-based models [4] [5] [6] [7]. Montgomery and Dietrich (1994) [8] developed a simple physically based model, based on digital terrain data, which couples a steady-state shallow saturated subsurface model with an infinite slope stability model. The steady-state model incorporates a scheme based on the formulation proposed by O'Loughlin (1986) [9] to simulate the topographic dependence of runoff generation during transient storm events in humid

environments. Tarolli et al. (2011) [10] used the QD-SLaM model to predict the spatial distribution of shallow landslide initiation.

The aim of this research is to investigate and evaluate the landslide hazard prone area, not only spatially but also temporally. Most of previous studies focused on either identification spatially distribution of landslide prone area or temporal prediction. In this study a coupled model between groundwater hydrology, surface hydrology and infinite slope model was used to find factor of safety in different rainfall periods, return period of landslide event and its duration based on statistical study of rainfall data.

## 2. Study Area

The study area located in the southern part of Seoul, between longitudes 126.9° to 127.04°E and latitudes 37.45° to 37.48°N as shown in Fig. 1. It covers approximately 6.8 km<sup>2</sup>. The elevation ranges from 20 m to 312 m amsl. The mountain is located at the center of a dense residential area, the hazard had a greater impact on the society compared to debris flows

that occurred in rural areas.

A record breaking heavy rainfall hits the whole Korea on June and July of 2011. Between 8:30 to 8:50 a.m. on July 27, 2011, many debris flows occurred simultaneously at Umyeon Mountain in Seoul. Saturated ground moved like a flow and hit residences and vehicles under the slope. The main cause of debris flow in Umyeon area was rainfall, which classify into two different ones based on the temporal variation. Firstly, the antecedent rainfall fell two weeks before the landslide event and is recorded as 463.0 mm. It fully saturated ground surface. Second, a heavy daily rainfall amounting 342.5 mm fell into the study area. It took about 74% of antecedent rainfall.

In the Umyeon Mountain, a total of 163 landslide initiation locations were mapped at 1:5, 000-scale topographic maps (Figure 1) and to produce a detailed and reliable landslide inventory map, extensive field survey and observations were performed. A landslide inventory map was prepared by consulting satellite images and web-based digital aerial photographs with 50-cm resolution provided by Naver ([www.map.naver.com](http://www.map.naver.com)) along with Global Positioning System (GPS) field surveys.

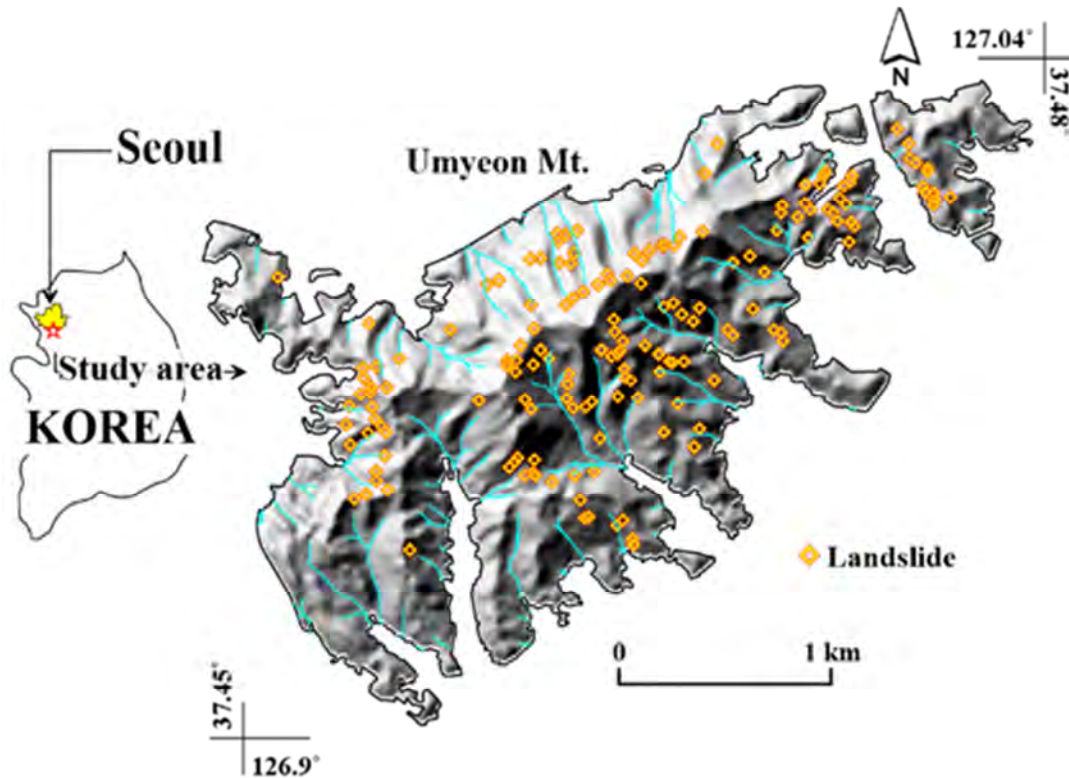


Figure 1. Location and landslide distribution in study area.

## 3. Methodology

### 3.1. Slope Stability Model

In this study, a basic infinite slope model proposed by Brunsden and Prior (1984) [11] was adopted to calculate factor of safety ( $FS$ ).

$$FS = \frac{c'}{\gamma Z \sin \alpha} + \left(1 - m \frac{\gamma_w}{\gamma}\right) \frac{\tan \phi'}{\tan \alpha} \quad (1)$$

where  $c'$  is the effective cohesion (kPa),  $\phi'$  is the effective friction angle (°),  $\alpha$  is slope angle (°),  $m$  represents the fractional depth of the water table with respect to the total slide depth and is called the saturation factor,  $\gamma$  is the material unit weight (kN/m<sup>3</sup>) and  $\gamma_w$  is the water unit weight

(kN/m<sup>3</sup>).

To predict the spatial distribution of soil saturation factor in response to a rainfall of specified duration, a quasi-dynamic wetness index (QDWI) was used. The QDWI is the ratio between the effective contributing area and the local slope [12]. The effective contributing area  $a(d)$  is the fraction of the total specific contributing area which contributes subsurface flow to the contour segment within a specified drainage period  $d$  corresponding to a rainfall duration. This is based on the hypothesis that all precipitation infiltrates and that vertically infiltrating volumes quickly redistribute and produce lateral subsurface flow. Under these assumption, the depth  $m$  of the top soil affected by the surface flow (measured orthogonal to the slope angle) is computed as follows [13]:

$$m = \min\left(\frac{r_o}{k_s \sin \alpha} a(d), Z\right) \quad (2)$$

where  $r_o$  is the constant rainfall rate (mmh<sup>-1</sup>),  $Z$ (m) is the soil depth,  $k_s$  (ms<sup>-1</sup>) is the saturated Hydraulic conductivity.

Coupling the groundwater model and the infinite slope stability model under the assumption that the failure plane is on the impeding layer provides a relationship for the critical rainfall rate  $rc(d)$ , in other words the rainfall rate required to trigger slope failure for the specific topographic element. The Eq. (1) can be modified as:

$$FS = \frac{c'}{\gamma z \sin \alpha} + \left[1 - \min\left(\frac{r_o}{k_s \sin \alpha} a(d), Z\right) \frac{\gamma_w}{\gamma}\right] \frac{\tan \phi'}{\tan \alpha} \quad (3)$$

Using Eq. (2), the factor of safety can be calculated in different saturation period of soil in hillslope. If  $FS$  is considered as an equilibrium state, this equation can be modified to calculate critical rainfall rate.

$$r_c(d) = \frac{k_s \sin \alpha}{a(d)} \left( \frac{\gamma}{\gamma_w} - \frac{\gamma \sin \alpha \cos \alpha - c'}{Z \cos^2 \alpha \tan \phi' \gamma_w} \right) \quad (4)$$

### 3.2. Combining Infinite Slope Model with Hydrological Model

Eq. (4) provides the critical rainfall rate for a precipitation of a given duration, thus offering a way to quantify the return time of the critical rainfall. The variability of storm intensity with duration for a specified frequency level is often represented by the intensity-duration-frequency (IDF) relation. A power function is often used to model the IDF relation [14]:

$$r_F(d) = \zeta_F d^{m_F-1} \quad (5)$$

where  $r_F$  is the rainfall rate which can be exceeded with a probability of  $(1-F)$ , and  $\zeta_F$  and  $m_F$  are model parameters. The scaling properties of the statistical moments of rainfall depths of different durations are used in this work to derive the IDF relationship [15].

Aronica et al. (2012) [16] showed that a generalized extreme value (GEV) simple scaling model described well the

distribution of annual maximum series of rainfall for the study region. The GEV simple scaling distribution of the rainfall rate  $r_F(d)$  can be determined as:

$$r_F(d) = \zeta_1 \cdot \left[1 - CV \cdot \frac{\sqrt{6}}{\pi} \cdot (\xi + y_{Tr})\right] \cdot d^{m-1} \quad (6)$$

where  $\xi$  is the Euler's constant (approximately 0.5772) and  $y_{Tr}$  can be derived by the following relation:

$$y_{Tr} = \ln\left(\ln\left(\frac{T_r}{T_r - 1}\right)\right) \quad (7)$$

where  $T_r$ , recurrence interval, corresponds to the exceedance probability  $(1-F)$ . The values of the parameters  $\zeta_1$  and  $m$  can be estimated by linear regression of mean values of annual maxima of precipitation depth against their durations, after log transformation. Combining Eqs. (4) and (6) yields the following equation for the value of  $y_{Tr}$ :

$$y_{Tr} = \frac{\pi}{\sqrt{6}} \cdot \frac{1}{CV} \left[1 - \frac{k_s \sin \alpha}{a(d)} \left(\frac{\gamma}{\gamma_w} - \frac{\gamma \sin \alpha \cos \alpha - c'}{Z \cos^2 \alpha \tan \phi' \gamma_w}\right) \frac{d^{1-m}}{\zeta_1}\right] - \xi \quad (8)$$

Although study area mainly covered by forest, in this study the vegetation surcharge and root cohesion were not considered in the analysis.

## 4. Results and Discussion

The proposed model was applied to depict the spatial and dynamics of  $FS$  values induced by heavy rainfall during 17 hr rainfall duration. Three cases were selected for the prediction based on soil saturation index in different periods as shown in Figure 2.

Case I is long term intensity considered as average value of 17hr rainfall duration with 19.1 mm/hr, case II is 15hr rainfall duration with average intensity 12mm/hr i.e. excluding last two hours extreme rainfall and in case III last two hours extreme average rainfall intensity i.e. 65.8 mm/hr was added to case II.

A DEM provide a topographic basis for the model [2]. The DEM was constructed using 1:5,000 scale LIDAR data, and a 10 × 10 m grid was used, giving a spatial resolution of the topographic data of 10 m.

Table 1 shows the input geotechnical data for model application. According to the unified soil classification system (USCS), the soil samples were characterized by non-plastic well- to poorly graded sand.

Table 1. Geotechnical properties.

Properties	Average value
Cohesion	2.14 (kPa)
Internal frictional angle	35.61
Density	1.68 (kg/m <sup>3</sup> )
Unit weight	17.7 (KN/m <sup>3</sup> )
Assumed soil depth	1 (m)

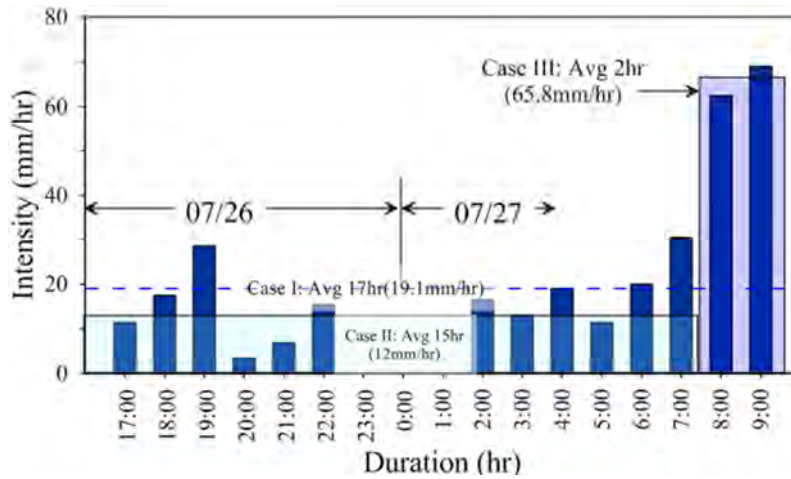


Figure 2. Input rainfall intensities in the model.

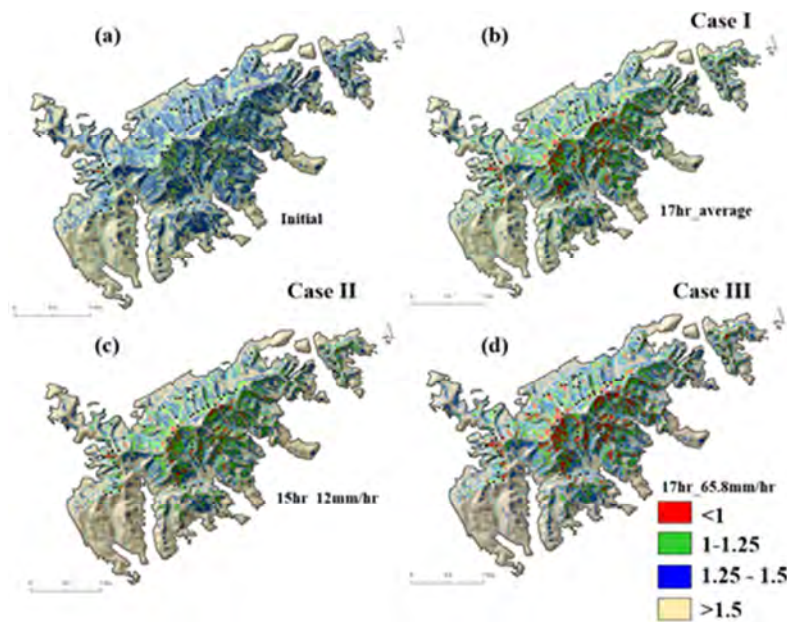


Figure 3. FS distribution: (a) initial condition, (b) Case I, (c) Case II and (d) Case III.

The model shows four classes of FS that varies from  $FS < 1$ ,  $1 - 1.25$ ,  $1.25 - 1.5$  and  $FS > 1.5$ , that were obtained using Eq. (3). When initial condition was subjected to difference cases, the FS distribution has changed (Figure 3). In case III, more area was flagged as high unstable zone.

In case III, 7.2% of terrain was classified with  $FS < 1$ . 39.9% landslides were flagged in this zone; 15.8% terrain was classified with  $FS 1 - 1.25$ , 32.52% landslides were depicted in this zone; 21.5% hillslope was classified with  $FS 1.25 - 1.5$  and this zone contained 18.4% landslide. Similarly, 55.5% area was classified as  $FS > 1.5$ , this zone contained 9.20% landslide.

The results from difference cases were compared with the model given in Eq. (1). The ROC plot shows that Traditional method has 64.9% accuracy whereas, Case III has 82.2% accuracy. The result in Case III has good accuracy (Figure 4). This showed that the model is good to apply to identify rainfall triggered shallow landslide.

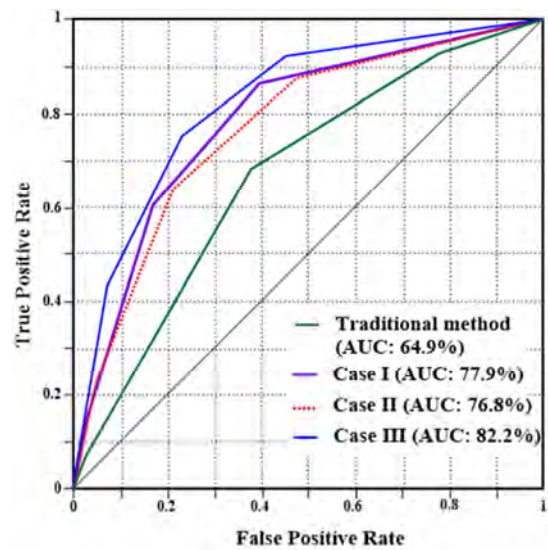


Figure 4. Model accuracy test using ROC.

*Table 2. Parameters estimated for Gumbel equation.*

Parameters	Value
$s_1$	68.5 mm
CV	0.382
m	0.506

Regional depth-duration-frequency relationship for the study area for return periods ranging from 10 to 300 yr. observed maxima for rainfall durations ranging from 1 to 6hr measured at the Seoul station. The analyzed values for parameters estimated for application of Gumbel equation is presented in Table 2, it shows the heavy rainfall regime in much stronger.

Duration and return period for  $FS=1$  was calculated using Eqs. (8) and (7). The duration of event map shows seven classes varies

from stable to unstable as shown in Figure 5. The observed landslides were distributed in the range from 3hrs to 12hrs rainfall duration. Similarly, the return period event maps shows seven classes same as duration map (Figure 6). The observed landslide inventory map was overlaid with return period map. It shows, most of the landslide return period distributed in the zone from 2–10 yrs to 50–100 yrs return period.

This results demonstrate the proposed model was successful in identifying the unstable areas under return critical rainfall and duration. The shallow landslide susceptibility incorporating rainfall statistics revealed several potentially affected areas by rainfall-triggered shallow landslides and debris flows, which corresponds to settlements.

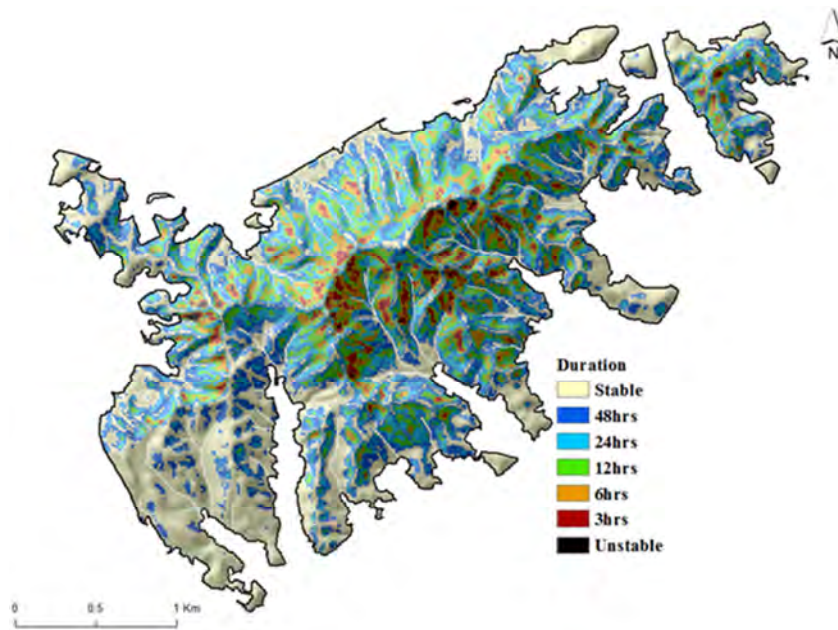


*Figure 5. Distribution of unstable zone in different rainfall duration.*

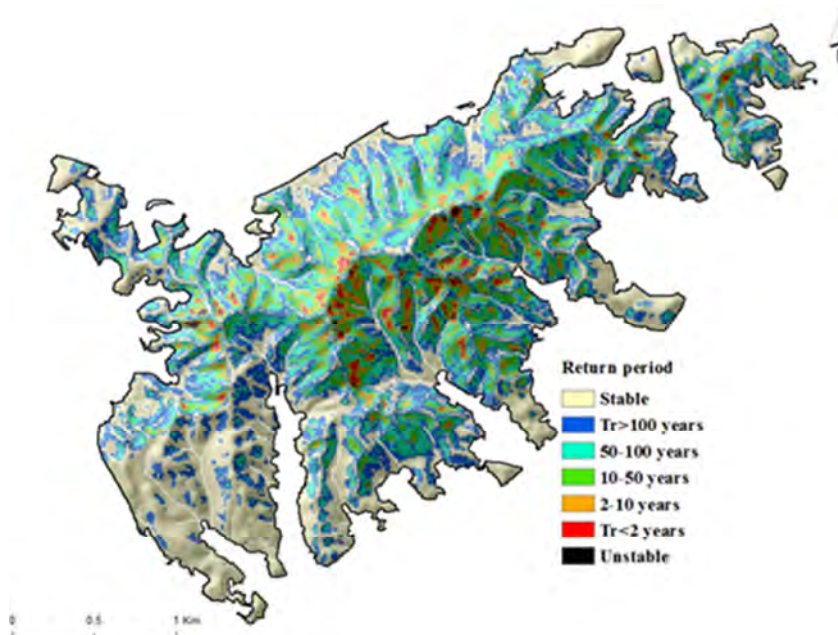


*Figure 6. Distribution of unstable zone in different rainfall return periods.*

## 5. Conclusions

The proposed model has been applied to the 6.8 km<sup>2</sup> Umyeon Mt. The model uses a 'quasi-dynamic' wetness index to predict the spatial distribution of soil saturation in response to a rainfall of specified duration. The approach provides a way to capture both topographic and climatic forcing on shallow landsliding. At each terrain element, the outputs from the model were distribution of FS, duration and critical rainfall return period. A combined approach of QDWI and infinite slope model was used to prepare landslide susceptibility maps of different durations i.e. considering 17hr duration with average rainfall intensity (case I), 15hr duration with average rainfall intensity (case II) and last 2hr duration and average intensity added in case II (case III). ROC plot was used to compare all cases. AUC of Case III has highest value, calculated as 82.2%. Whereas, performance of infinite slope model in fully saturated condition is 64.9%.

The return period and duration maps were prepared using coupling simple scaling approach, the Gumbel-derive F-quantile. Most of the landslide flagged in 3hrs-12hrs duration and 2-100 yrs return periods.

A coupled model of infinite model and rainfall is important for hazard mitigation in a mountainous area.

## Acknowledgements

This research was supported by the Public Welfare and Safety Research Program through the National Research Foundation of Korea (NRF), funded by the Ministry of Science, ICT, and Future Planning (grant No. 2012M3A2A1050977), a grant (13SCIPS04) from Smart Civil Infrastructure Research Program funded by Ministry of Land, Infrastructure and Transport (MOLIT) of Korea government and Korea Agency for Infrastructure Technology Advancement (KAIA) and the Brain Korea 21 Plus (BK 21 Plus).

## References

- [1] Chung Y. S., Yoon M. B., and Kim H. S. (2004) On climate variations and changes observed in South Korea. *Climatic Change*. Vol. 66. pp. 151–161.
- [2] Pradhan A. M. S. and Kim Y. T. (2015) Application and comparison of shallow landslide susceptibility models in weathered granite soil under extreme rainfall events. *Environmental Earth Sciences*. Vol: 73, No. 9. pp. 5761–5771.
- [3] Guzzetti F., Reichenbach P., Cardinali M., Galli M., and Ardizzone F. (2005) Probabilistic landslide hazard assessment at the basin scale. *Geomorphology*. Vol. 72, pp. 272–299.
- [4] Carrara A., Cardinali M., Detti R., Guzzetti F., Pasqui V., and Reichenbach P. (1991) GIS techniques and statistical models in evaluating landslide hazard. *Earth Surf. Processes Landforms*, Vol. 16. pp. 427–445.
- [5] Pradhan A. M. S., Kang H. S., Lee J. S., Kim Y. T. (2017) An ensemble landslide hazard model incorporating rainfall threshold for Mt. Umyeon, South Korea. *Bulletin of Engineering Geology and the Environment*, pp. 1-16. (online first).
- [6] Pradhan A. M. S., Kim Y. T. (2017) GIS-based landslide susceptibility model considering effective contributing area for drainage time. *Geocarto International*, pp. 1-20. (online first).
- [7] Saro L., Woo J. S., Kwan-Young O., Mounj-Jin L. (2016) The spatial prediction of landslide susceptibility applying artificial neural network and logistic regression models: A case study of Inje, Korea. *Open Geosciences*, Vol. 8, No. 1. pp. 117-132.
- [8] Montgomery D. R. and Dietrich W. E. (1994): A physically based model for the topographic control on shallow landsliding. *Water Resources Research* Vol. 30. pp. 1153–1171.
- [9] O'Loughlin E. M. (1986) Prediction of surface saturation zones in natural catchments by topographic analysis, *Water Resources Research*, Vol. 22, No. 5. pp. 794–804.
- [10] Tarolli P., Borga M., Chang K. T., Chiang S. H. (2011). Modeling shallow landsliding susceptibility by incorporating heavy rainfall statistical properties. *Geomorphology*. Vol. 133. No. 3. pp. 199-211.
- [11] Brunsdon, D. and Prior, D. B. (1984) Slope Stability. New York, Wiley, pp. 620.
- [12] Borga, M., Dalla Fontana, G., and Cazorzi, F. (2002) Analysis of topographic and climatic control on rainfall-triggered shallow landsliding using a quasi-dynamic wetness index, *J. Hydrol.*, Vol. 268, pp. 56–71.
- [13] Barling, D. B., Moore, I. D., and Grayson, R. B. (1994) A quasi-dynamic wetness index for characterizing the spatial distribution of zones of surface saturation and soil water content, *Water Resour. Res.*, Vol. 30, pp. 1029–1044.
- [14] Koutsoyiannis, D., Kozonis, D., and Manetas, A. (1998) A mathematical framework for studying rainfall intensity-duration-frequency relationships, *J. Hydrol.*, Vol. 206. pp. 118–135.
- [15] Ceresetti, D., Molinié, G., and Creutin, J.-D. (2010) Scaling properties of heavy rainfall at short duration: A regional analysis, *Water Resour. Res.*, Vol. 46, W09531, doi: 10.1029/2009WR008603.
- [16] Aronica, G. T., Brigandí, G., and Morey, N. (2012) Flash floods and debris flow in the city area of Messina, north-east part of Sicily, Italy in October 2009: the case of the Giampileri catchment, *Nat. Hazards Earth Syst. Sci.*, Vol. 12, pp. 1295–1309.